



## Ultrafast softening in InMnAs

J. Wang<sup>a</sup>, G.A. Khodaparast<sup>a</sup>, J. Kono<sup>a,\*</sup>, T. Slupinski<sup>b,1</sup>, A. Oiwa<sup>b,2</sup>, H. Munekata<sup>b</sup>

<sup>a</sup>Department of Electrical and Computer Engineering, Rice Quantum Institute, Center for Nanoscale Science and Technology, Rice University, Houston, TX 77005, USA

<sup>b</sup>Imaging Science and Engineering Laboratory, Tokyo Institute of Technology, Yokohama, Kanagawa 226-8503, Japan

### Abstract

We have used two-color time-resolved magneto-optical Kerr effect spectroscopy to manipulate and detect dynamic processes of spin/magnetic order in a ferromagnetic semiconductor InMnAs. We observed ultrafast photo-induced “softening” (i.e., transient decrease of coercivity) due to spin-polarized transient carriers. This transient softening persists only during the carrier lifetime ( $\sim 2$  ps) and returns to its original value as soon as the carriers recombine to disappear. Our data clearly demonstrates that magnetic properties, e.g., coercivity, can be strongly and reversibly modified in an ultrafast manner. We attribute the origin of this unusual phenomenon to carrier-mediated ferromagnetic exchange interactions between Mn ions. We discuss the dependence of data on the pump polarization, pump intensity, and sample temperature. Our observation opens up new possibilities for ultrafast optical manipulation of ferromagnetic order as well as providing a new avenue for studying the dynamics of long-range collective order in strongly correlated many-body systems.

© 2003 Elsevier B.V. All rights reserved.

PACS: 78.20.-e; 78.20.Jq; 42.50.Md; 78.30.Fs; 78.47.+p

Keywords: Ferromagnetic semiconductors; Magneto-optical Kerr effect; Ultrafast spectroscopy

### 1. Introduction

Recent experiments on III–V magnetic semiconductors have revealed unique properties that may find application in future “multifunctional” devices—i.e., semiconductor devices that work as electronic, photonic, and magnetic devices, simultaneously. The co-existence and mutual interaction of free carriers (i.e.,

holes) and localized magnetic moments (i.e., Mn ions) make it possible to control magnetic properties by applied dc electric fields [1] and CW light illumination [2–4]. Namely, ferromagnetism in III–V ferromagnetic semiconductors such as InMnAs [5,6] and GaMnAs [7] is *carrier-mediated*, and their magnetic characteristics are sensitive functions of carrier density. Hence, carrier-density-tuning is the key to the successful manipulation of ferromagnetism either electrically or optically, as clearly shown in recent demonstrations [1–4].

However, how one can manipulate magnetic order of ferromagnetic semiconductors in an *ultrafast manner* is still an open question although it is of significant current interest both from scientific and

\* Corresponding author.

E-mail address: [kono@rice.edu](mailto:kono@rice.edu) (J. Kono).

URL: <http://www.ece.rice.edu/~kono>.

<sup>1</sup> Present address: Institute of Experimental Physics, Warsaw University, Hoza 69, 00-681 Warsaw, Poland.

<sup>2</sup> Present address: PRESTO, Japan Science and Technology Corporation, 4-1-8 Honcho, Kawaguchi, 332-0012, Japan.

technological viewpoints. The interplay between photogenerated transient carriers created by ultrashort laser pulses and carrier-induced ferromagnetism in III–V ferromagnetic semiconductors paves a natural way towards such a goal. On one hand, pumping semiconductors with ultrashort laser pulses results in a large density of spin-coherent carriers, which should be able to strongly and transiently affect exchange interactions between Mn ions and, in turn, modify ferromagnetic order. On the other hand, study of the effects of *transient* carriers on magnetism will be very useful for the microscopic understanding of the origin of carrier-induced ferromagnetism, which is still controversial. This should provide us with valuable information on how magnetic characteristics would change as functions of the ratio of the hole density to the Mn density in a single sample, which is a crucial parameter in the various existing theoretical models. It is also interesting to note that many time-domain optical studies of itinerant ferromagnets have been performed recently, which revealed a variety of new dynamic phenomena (for a review, see, e.g., Ref. [8]; see also Refs. [9–17]), although exactly how a laser pulse can effectively change the long-range magnetic order on a femtosecond time scale is highly controversial [15–18]. The coexistence of long-range collective order, short-range Coulomb correlations between carriers, and strong exchange couplings between them via s–d and p–d exchange interactions make III–V ferromagnetic semiconductors fascinating system for studying ferromagnetic dynamic processes. However, their transient properties are mostly unexplored.

Here, we report on our discovery of *ultrafast softening* (i.e., a transient photo-induced decrease of coercivity) in ferromagnetic InMnAs/GaSb heterostructures using two-color time-resolved magneto-optical Kerr (MOKE) spectroscopy. We observed that photogenerated transient carriers significantly *decrease* the coercivity ( $H_c$ ) while almost sustaining the saturation magnetization. We attribute this phenomenon to the carrier-enhanced Mn–Mn exchange interaction, which decreases the domain wall energy (increases the magnetic polaron diameter) in the domain picture (particle picture). We also performed simultaneous measurements of MOKE angle and reflectivity for examining spin and charge dynamics separately, which supports our interpretation that the fast, subpicosecond switching of the soften-

ing process is due to the ultrashort carrier lifetimes in ferromagnetic semiconductors. Furthermore, coherent optical spin injection using different senses of circular polarization led to different signs for the net MOKE changes induced by the pump. Finally, the temperature and pump intensity dependences of these effects will be shown and discussed.

## 2. Experimental details

We performed two-color time-resolved MOKE spectroscopy experiments using femtosecond ( $\sim 150$  fs) pulses of midinfrared (MIR) and near-infrared (NIR) radiation. Fig. 1(a) shows a schematic diagram of the experimental setup, which were described previously [19]. The source of intense MIR pulses was an optical parametric amplifier (OPA) pumped by a Ti:Sapphire-based regenerative amplifier (Model CPA-2010, Clark-MXR, Inc., 7300 West Huron River Drive, Dexter, MI 48130). The OPA was able to produce tunable and intense radiation from 522 nm to 20  $\mu\text{m}$  using different mixing crystals. The CPA produced pulses of NIR radiation with a wavelength of 775 nm, a pulse energy of  $\sim 1$  mJ, and a pulse duration of  $\sim 140$  fs at a tunable repetition rate of 50 Hz–1 kHz. We used a very small fraction ( $\sim 10^{-5}$ ) of the CPA beam as a probe and the output beam from the OPA tuned to 2  $\mu\text{m}$  as the pump. The two beams were made collinear by a non-polarizing beam splitter and then focused onto the sample mounted inside a superconducting magnet with optical windows. We recorded the intensity difference of the s- and p-components of the reflected NIR beam using a balanced differential detector as well as its total intensity as functions of time delay and magnetic field. The signal from the balanced detectors, which was proportional to the induced MOKE angle change, was fed into a lock-in amplifier or a boxcar integrator. Data was recorded by a computer using average acquisition or shot by shot acquisition.

Fig. 1(b) shows a schematic band diagram of the InMnAs/GaSb sample studied. Surface pinning of the Fermi energy and the type-II ‘broken-gap’ alignment between InMnAs and GaSb produces large band bending. This bending together with Mn doping creates two pockets for holes. Also shown in Fig. 1(b) is the selective pumping scheme we used. At the pump

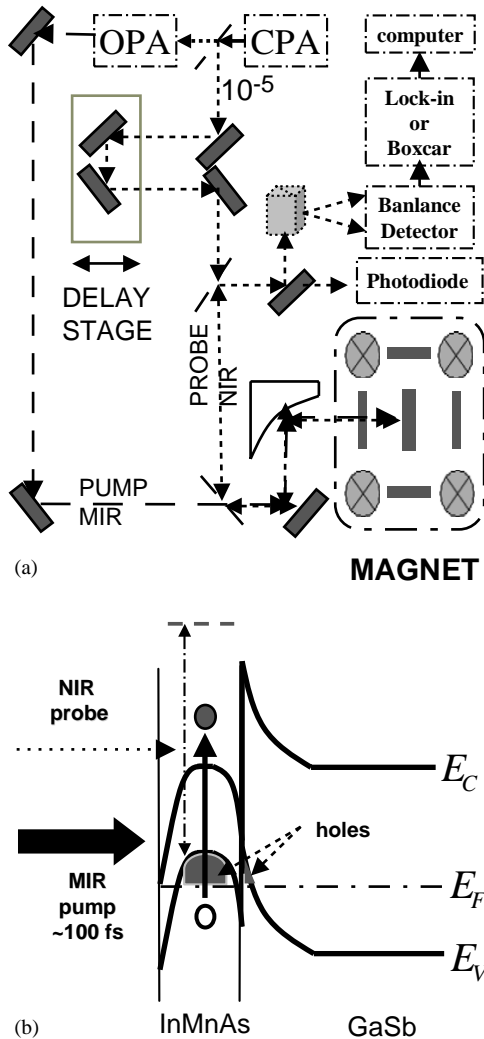


Fig. 1. (a) Schematic diagram for the two-color time-resolved MOKE spectroscopy experiments. (b) Band diagram of the InMnAs/GaSb sample together with our pumping and probing scheme. We selectively pump the sample with MIR pulses with photon energy larger than the InMnAs band gap but smaller than the GaSb band gap, creating transient carriers only within the magnetic layer. Weaker near-infrared pulses, with photon energy far above the quasi Fermi energy of optical excitation, probe the time-dependent ferromagnetism via Kerr rotation.

wavelength ( $2 \mu\text{m}$ ), the photon energy ( $0.62 \text{ eV}$ ) was smaller than the band gaps of GaSb ( $0.812 \text{ eV}$ ) and GaAs ( $1.519 \text{ eV}$ ) but larger than that of InMnAs ( $\sim 0.42 \text{ eV}$ ), so the pump created carriers only in the InMnAs layer. Under our pumping conditions, the

maximum density of photocreated carriers are estimated to be comparable to or larger than the background carrier density ( $\sim 10^{19} \text{ cm}^{-3}$ ), and, hence, significant modifications in exchange interactions can be expected.

The sample mainly studied was an InMnAs/GaSb single heterostructure with a Curie temperature ( $T_c$ ) of  $55 \text{ K}$ , consisting of a  $25 \text{ nm}$  thick  $\text{In}_{0.91}\text{Mn}_{0.09}\text{As}$  magnetic layer and an  $820 \text{ nm}$  thick GaSb buffer layer grown on a semiinsulating GaAs (100) substrate. Its room temperature hole density and mobility were  $1.1 \times 10^{19} \text{ cm}^{-3}$  and  $323 \text{ cm}^2/\text{Vs}$ , respectively, estimated from Hall measurements. The sample was grown by low temperature molecular beam epitaxy (growth conditions described previously [20]) and then annealed at  $250^\circ\text{C}$ , which increased the  $T_c$  by  $\sim 10 \text{ K}$  [21,22]. The magnetization easy axis was perpendicular to the epilayer due to the strain-induced structural anisotropy caused by the lattice mismatch between InMnAs and GaSb (InMnAs was under tensile strain). This allowed us to observe ferromagnetic hysteresis loops in the polar Kerr configuration.

### 3. Experimental results

Before showing data related to ultrafast photo-induced changes in ferromagnetic order, we first present CW data. Fig. 2 shows CW magnetic circular dichroism data taken for the sample at  $10$ ,  $35$ ,  $45$  and  $55 \text{ K}$ . As can be seen clearly, raising the lattice temperature results in dramatic loop shrinkage *both horizontally and vertically*.

Typical data showing the ultrafast photo-induced softening process are presented in Fig. 3. Here, two magnetic-field ( $B$ )-scans exhibiting ferromagnetic hysteresis loops at  $20 \text{ K}$  are plotted together for  $-4 \text{ ps}$  and  $430 \text{ fs}$  time delays, respectively. The pump beam was circularly polarized. The data at  $-4 \text{ ps}$  delay (Fig. 3(a)) shows a hysteresis loop with a finite coercivity ( $\sim 1 \text{ mT}$ ). However, at timing zero (Fig. 3(b)), when the pump and probe coincide, the hysteresis loop is totally suppressed in the horizontal direction, i.e., the coercivity is almost zero. It is important to note that the ferromagnetic hysteresis loop at timing zero shows almost no change (or slightly increase  $< 10\%$ , if any) in the vertical height of the loop within the sensitivity of our setup.

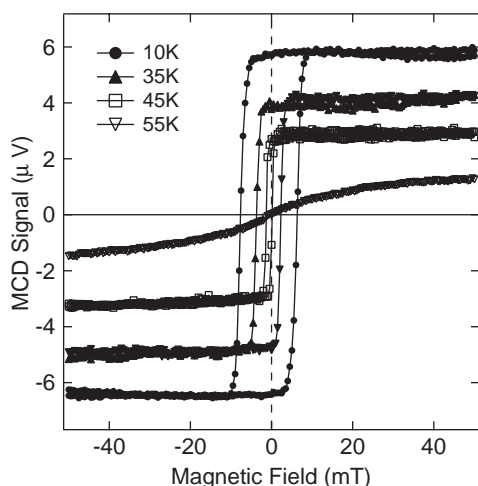


Fig. 2. CW magnetic circular dichroism data taken at four different temperatures (10, 35, 45, and 55 K).

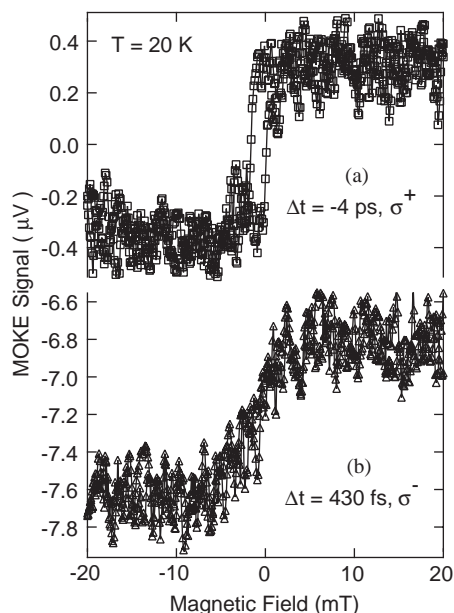


Fig. 3. Ultrafast photo-induced softening. MOKE signal vs. magnetic field for two different time delays. (1) Black squares:  $-4$  ps; (2) black triangles:  $430$  fs. A ferromagnetic hysteresis loop is clearly seen only at negative time delay. At  $430$  fs, the loop is nearly destroyed in the horizontal direction, i.e., coercivity is almost zero. In addition, note that this curve is not intentionally offset; namely, vertical shift of ferromagnetic hysteresis loops is a real effect induced by the pump.

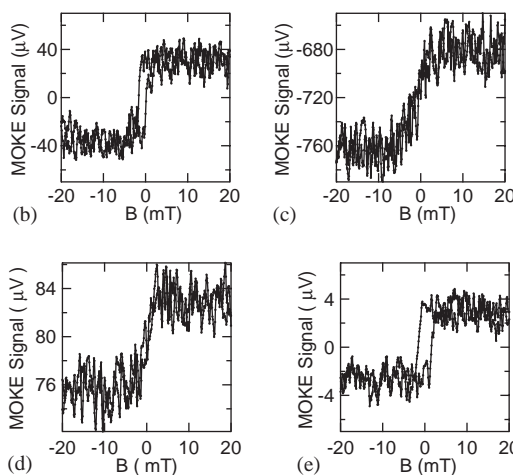
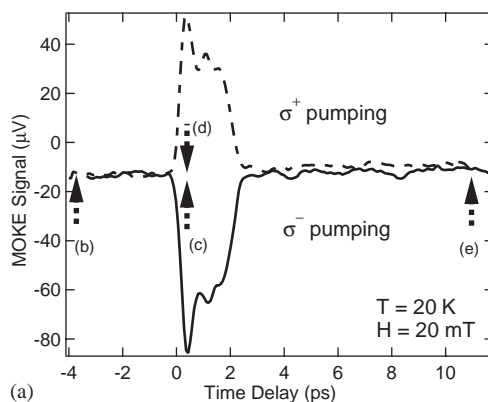


Fig. 4. Detailed MOKE dynamics. (a) Time scan at  $-0.02$  T and  $20$  K. Black circles: The  $2\text{-}\mu\text{m}$  pump was circularly polarized ( $\sigma^-$ ); Red triangle: The  $2\text{-}\mu\text{m}$  pump was circularly polarized ( $\sigma^+$ ). The probe wavelength was  $775$  nm. A  $\sim 2$  ps photo-induced MOKE response is observed in both case with opposite sign of signal. (b)–(e): MOKE signals vs. field at different time delays, corresponding to the specific positions shown in (a). (b)  $-4$  ps,  $\sigma^-$ ; (c)  $\sim 500$  fs,  $\sigma^-$ ; (d)  $\sim 500$  fs,  $\sigma^+$ ; (e)  $11$  ps,  $\sigma^-$ .

Fig. 4 plots detailed photo-induced magnetization dynamics. Fig. 4(a) shows two traces representing the pump-induced MOKE signal change versus time delay taken under the excitation of the MIR pump with two opposite senses of circular polarization, i.e.,  $\sigma^+$  and  $\sigma^-$ . An ultrafast photo-induced response is clearly observed in both cases. As demonstrated here, opposite polarizations result in *opposite signs* of the photo-induced MOKE change. Ferromagnetic loops are plotted in Figs. 4(b)–(e), which correspond to the fixed time delays indicated in Fig. 4(a). Again,

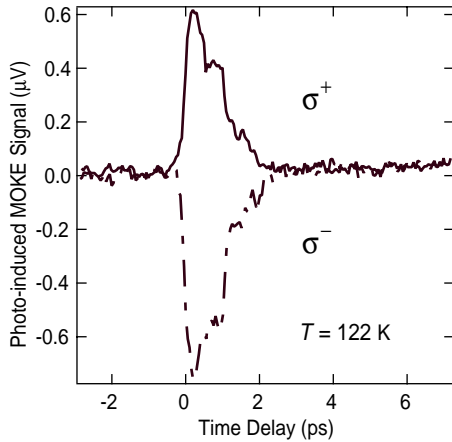


Fig. 5. Photo-induced MOKE signal vs. time delay for an InMnAs/GaSb heterostructure with a Curie temperature of 55 K, taken at 122 K under pumping with circularly polarized MIR radiation.

at timing zero (Figs. 4(c) and (d)), the loop is collapsed horizontally. It can be seen that such softening lasts only for a very short time,  $\sim 2$  ps. As soon as the photo-induced MOKE signal disappears (see Fig. 4(a)), a loop reappears with the original  $H_c$  recovered (see Fig. 4(e)). We refer to the observed transient horizontal quenching of the ferromagnetic hysteresis loop as ultrafast photo-induced softening. Note that the ferromagnetic hysteresis loops shift to opposite directions under different pumping conditions, i.e.,  $\sigma^+$  and  $\sigma^-$ .

To further understand the nature of the polarization-dependent ultrafast vertical shift of the MOKE signal, we did the same measurements at elevated temperatures. As an example, data taken at 122 K is shown in Fig. 5. Here, again, we see opposite signs for  $\sigma^+$  and  $\sigma^-$  polarizations. Note that the Curie temperature of this sample is 55 K. These facts lead us to believe that the polarization-dependent vertical shifts of the MOKE signals are due to the coherent carrier spins. We will provide a more discussion on this in the next section.

Finally, we determined the charge carrier lifetime to be  $\sim 1$  ps by a two-color pump-probe method, i.e., pumping with the MIR beam to create carriers in the InMnAs layer and probing through the reflectivity change of the NIR beam. As an example, Fig. 6 shows differential reflectivity vs. time delay, which exhibits two main features: First, the initial

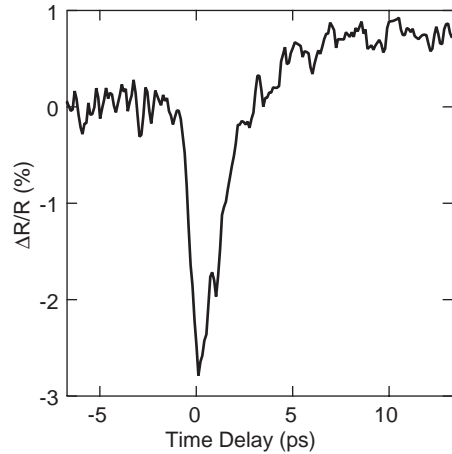


Fig. 6. Two-color time-resolved transient reflectivity measurements of InMnAs. The reflectivity of NIR probe was plotted vs. time delay under MIR pumping, showing an extremely fast decay of charge carriers.

signal (time delay less than 1 ps) is negative, i.e., the reflectivity decreases transiently. Second, the sign of differential reflectivity rapidly changes to positive and subsequently decays slowly ( $\sim$  several hundred ps). Similar behaviors have been observed in low temperature MBE (LT-MBE) grown III–V semiconductors such as GaAs, InP, and InGaP [23,24]. The initial quick disappearance of the negative induced reflectivity has been attributed to the decrease of the carrier density, which correspond to the carrier lifetime. The short charge lifetime is due to anti-site defects introduced during low-temperature MBE growth [25], which provide extra defect states within the band gap and trap photogenerated transient carriers. In addition, the slow recovery of the positive signal in the transient reflectivity is the result of the reexcitation of the trapped carriers.

#### 4. Discussion

First, let us discuss the origin of the ultrafast signal in Fig. 4(a) (i.e., the vertical shifts). We can exclude nonlinear optical effects such as state filling, band filling, and band gap renormalization since the two-color nature of the current measurements allows us to decouple the photogenerated carriers from the energy levels probed. Namely, the quasi-Fermi level of the optically excited carrier system is too low to affect the

probe. An important fact to note is that all data indicate that no magnetization change accompanied the vertical shifts within the sensitivity of our experiment. Furthermore, as clearly shown in Fig. 5, we observe similar effects at temperature much higher than the Curie temperatures. Therefore, we conclude that the vertical shifts are not due to any change related to ferromagnetism and the coherent spin polarization of the photogenerated carriers is the origin of the ultrafast signal in the time scans, which leads to the vertical shift of ferromagnetic hysteresis loop. Thus, such time scans provide a direct measure of the spin lifetime of photogenerated carrier.

We believe that carrier-enhanced exchange coupling between Mn ions is at the core of the observed ultrafast photo-induced softening. The phenomenon is essentially the same as what has been observed in the CW work on the same systems [3,26,27] except for the very different time scales. One possible scenario is in terms of domain walls [3]. Namely, creation of a large population of transient holes breaks the original balance between the exchange energy and the anisotropy energy (the latter was found to be independent of carrier density [3]). The dominance of the former results in an increase in domain wall thickness and a decrease in domain wall energy. This reduces the magnetic field required to achieve magnetization reversal, i.e., coercivity is decreased. Another possible mechanism involves the magnetic rotation of single-domain particles known as magnetic polarons. In an assembly of such particles, the interaction field among the particles is opposite to the particle magnetization and thus helps to reverse the particles. This gives rise to a reduction of the coercive field needed for magnetization reversal compared to that of a single particle. The size of the interaction field can be expressed as  $ApM(p)$ , where  $A$ ,  $p$ , and  $M(p)$  are the proportionality constant, the packing fraction, and single particle magnetization [28]. A large enhancement of the exchange coupling leads to the enlargement of magnetic polarons and thus increases the packing fraction  $p$  and single particle magnetization  $M(p)$ . This increases the interaction field and reduces the coercive force. As soon as the transient photogenerated carriers are gone, the original value of the coercivity field is recovered. This is consistent with the notion that the extremely short-lived photogenerated carriers are the cause of ultrafast photo-induced softening.

## 5. Summary

Using a novel two-color time-resolved MOKE spectroscopy technique, we have demonstrated ultrafast photo-induced softening, i.e., a transient coercivity decrease, in an InMnAs/GaSb ferromagnetic semiconductor heterostructure. We found surprisingly fast, subpicosecond switching due to ultrashort carrier lifetimes in ferromagnetic semiconductor InMnAs, exceeding the fundamental time limitation set by the thermo-magnetic process. The extremely fast decay and recovery of the observed ferromagnetic softening process differentiates itself from any known ultrafast processes in ferromagnetic systems. We expect that this discovery can have tremendous technological impact. For instance, one can imagine realizing thermal-free, ultrafast data writing in magneto-optical recording, or developing an ultrafast gating scheme in a multifunctional semiconductor device that can simultaneously process and store information encoded in the spin degree of freedom of electrons.

## Acknowledgements

This work was supported by DARPA through Grant No. MDA972-00-1-0034 (SPINS) and NSF through Grant Nos. DMR-0134058 and INT-0221704. H.M. acknowledges partial support from Scientific Research in Priority Areas “Semiconductor Nanospintronics” (2002) of the Ministry of Education, Science, and Technology, Japan.

## References

- [1] H. Ohno, D. Chiba, F. Matsukura, T. Omiya, E. Abe, T. Dietl, Y. Ohno, K. Ohtani, *Nature* 408 (2000) 944.
- [2] S. Koshihara, A. Oiwa, M. Hirasawa, S. Katsumoto, Y. Iye, C. Urano, H. Takagi, H. Munekata, *Phys. Rev. Lett.* 78 (1997) 4617.
- [3] A. Oiwa, T. Slupinski, H. Munekata, *Appl. Phys. Lett.* 78 (2001) 518.
- [4] A. Oiwa, Y. Mitsumori, R. Moriya, T. Slupinski, H. Munekata, *Phys. Rev. Lett.* 88 (2002) 137202.
- [5] H. Munekata, H. Ohno, S. von Molnar, A. Segmuller, L.L. Chang, L. Esaki, *Phys. Rev. Lett.* 63 (1989) 1849; H. Ohno, H. Munekata, T. Penney, S. von Molnar, L.L. Chang, *Phys. Rev. Lett.* 68 (1992) 2664.
- [6] H. Munekata, A. Zaslavsky, P. Fumagalli, R.J. Gambino, *Appl. Phys. Lett.* 63 (1993) 2929.

- [7] H. Ohno, A. Shen, F. Matsukura, A. Oiwa, A. Endo, S. Katsumoto, Y. Iye, *Appl. Phys. Lett.* 69 (1996) 363.
- [8] G. Zhang, W. Hübner, E. Beaurepaire, J.-Y. Bigot, in: B. Hillebrands, K. Ounadjela (Eds.), *Spin Dynamics in Confined Magnetic Structures I*, Springer, Berlin, 2002, pp. 245–288.
- [9] E. Beaurepaire, J.-C. Merle, A. Daunois, J.-Y. Bigot, *Phys. Rev. Lett.* 76 (1996) 4250.
- [10] J. Hohlfeld, E. Matthias, R. Knorren, K.H. Bennemann, *Phys. Rev. Lett.* 78 (1997) 4861.
- [11] A. Scholl, L. Baumgarten, R. Jacquemin, W. Eberhardt, *Phys. Rev. Lett.* 79 (1997) 5146.
- [12] M. Aeschlimann, M. Bauer, S. Pawlik, W. Weber, R. Burgermeister, D. Oberli, H.C. Siegmann, *Phys. Rev. Lett.* 79 (1997) 5158.
- [13] G. Ju, A. Vertikov, A.V. Nurmikko, C. Canady, G. Xiao, R.F.C. Farrow, A. Cebollada, *Phys. Rev. B* 57 (1998) R700.
- [14] E. Beaurepaire, M. Maret, V. Halté, J.-C. Merle, A. Daunois, J.-Y. Bigot, *Phys. Rev. B* 58 (1998) 12134.
- [15] J. Güdde, U. Conrad, V. Jähnke, J. Hohlfeld, E. Matthias, *Phys. Rev. B* 59 (1999) R6608.
- [16] B. Koopmans, M. van Kampen, J.T. Kohlhepp, W.J.M. de Jonge, *Phys. Rev. Lett.* 85 (2000) 844.
- [17] L. Guidoni, E. Beaurepaire, J.-Y. Bigot, *Phys. Rev. Lett.* 89 (2002) 017401.
- [18] G.P. Zhang, W. Hübner, *Phys. Rev. Lett.* 85 (2000) 3025.
- [19] J. Wang, G.A. Khodaparast, J. Kono, T. Slupinski, A. Oiwa, H. Munekata, *J. Supercond.* 16 (2003) 373.
- [20] T. Slupinski, A. Oiwa, S. Yanagi, H. Munekata, *J. Cryst. Growth* 237–239 (2002) 1326.
- [21] T. Hayashi, Y. Hashimoto, S. Katsumoto, Y. Iye, *Appl. Phys. Lett.* 78 (2001) 1691.
- [22] S.J. Potashnik, K.C. Ku, S.H. Chun, J.J. Berry, N. Samarth, P. Schiffer, *Appl. Phys. Lett.* 79 (2001) 1495.
- [23] S. Gupta, M.Y. Frankel, J.A. Valdmanis, J.F. Whitaker, F.W. Smith, A.R. Calawa, *Appl. Phys. Lett.* 59 (1989) 3276.
- [24] U. Siegner, R. Fluck, G. Zhang, U. Keller, *Appl. Phys. Lett.* 69 (1996) 2566.
- [25] F.W. Smith, H.Q. Le, V. Diadiuk, M.A. Hollis, A.R. Calawa, S. Gupta, M. Frankel, D.R. Dykaar, G.A. Mourou, T.Y. Hsiang, *Appl. Phys. Lett.* 54 (1989) 890.
- [26] A. Oiwa, T. Slupinski, H. Munekata, *Physica E* 10 (2001) 201.
- [27] H. Munekata, A. Oiwa, T. Slupinski, *Physica E* 13 (2002) 516.
- [28] D.F. Eldridge, *J. Appl. Phys.* 32 (1961) 247S.